*Journal of Reproduction and Development, Vol. 70, No 5, 2024*

**Technology Report**

# Zinc transporter *ZnT3/Slc30a3* has a potential role in zinc ion influx in mouse oocytes

**Atsuko KAGEYAMA[1)], Jumpei TERAKAWA[2, 3)], Shunsuke TAKARABE[1, 3)], Hibiki SUGITA[1, 3)], Yui KAWATA[1)], Junya ITO[1, 3, 4)] and Naomi KASHIWAZAKI[1, 3)]**

[1)]*Laboratory of Animal Reproduction, School of Veterinary Medicine, Azabu University, Sagamihara 252-5201, Japan*
[2)]*Laboratory of Toxicology, School of Veterinary Medicine, Azabu University, Sagamihara 252-5201, Japan*
[3)]*Graduate School of Veterinary Sciences, Azabu University, Sagamihara 252-5201, Japan*
[4)]*Center for Human and Animal Symbiosis Science, Azabu University, Sagamihara 252-5201, Japan*

Abstract. Zinc is an essential trace element for various physiological functions, including reproduction. The influx/efflux of zinc ions is regulated by zinc transporters (Zip1–14 and ZnT1–8, 10). However, the precise roles of zinc transporters and zinc dynamics in reproductive functions are unknown. In this study, *ZnT3*/*Slc30a3* gene knockout (KO) mice were used to analyze the role of *ZnT3*. In *ZnT3* KO mice, intracellular zinc ions in oocytes/zygotes were significantly reduced compared to those in controls, and free zinc ions did not accumulate in the oocyte cytoplasm. However, fertilization of these oocytes and the average litter size were comparable to those of control mice. Our results suggest that ZnT3 plays an important role in the accumulation of zinc ions in oocytes but not in the developmental ability of mice. *ZnT3* KO mice will be useful for examining zinc dynamics in oocytes and other tissues.
Key words: Fertility, Zinc, Zinc transporter, ZnT3/Slc30a3

(**J. Reprod. Dev. 70:** 338–342, 2024)

Zinc is the second most abundant essential trace element in the body. Zinc ions are essential for the activation of numerous enzymes involved in metabolic pathways and intracellular signaling, which are critical for maintaining vital cellular functions[1]. Zinc also plays a role in cell growth, cell division, and gene expression [2, 3]. Recent studies have shown that zinc plays a significant role in reproductive functions, including sperm formation, oocyte maturation, and fertilization, highlighting the need for adequate zinc intake for reproductive health [4–6].

Transient release of zinc ions, known as "zinc sparks," occurs shortly after a series of calcium oscillations during mammalian fertilization [7]. Zinc sparks have been observed not only in mice [7], but also in cows [8], non-human primates [7], humans [9], and even African clawed frogs [10], indicating their evolutionary importance. Zinc sparks reduce sperm motility and prevent polyspermy [11], highlighting the critical role of zinc ion homeostasis in germ cells.

Zinc ion homeostasis is maintained by two families of zinc transporters [12]: the ZIP (SLC39) family, which regulates zinc uptake into the cytoplasm, and the ZnT (SLC30) family, which regulates zinc efflux [13, 14]. Fourteen *Zip* genes (*Slc39a1-14/Zip1-14*) and nine *ZnT* genes (*Slc30a1-8, 10/ZnT1-8, 10*) have been identified in humans and mice [13, 14]. ZnT9 is now found to be the same molecule as the nuclear receptor coactivator GAC63 and has been excluded from the ZnT classification [15]. ZIP6 and ZIP10 are involved in zinc uptake in oocytes [14, 16], and inhibition of these transporters affects zinc levels, leading to abnormalities in meiotic progression [14]. However, the functions of ZnT transporters in oocytes remain unknown. In this study, we focused on *ZnT3/Slc30a3*, a highly expressed zinc transporter in mouse oocytes, and investigated the role of ZnT3 in reproductive function by generating knockout mice.

First, we confirmed the expression pattern of ZnT3 in mouse ovarian follicles. Our results showed that ZnT3 was expressed in oocytes at all follicular stages, from the primordial to antral follicles (Fig. 1A). ZnT3 expression was found in the cytoplasm but not on the plasma membrane surface, which may be related to zinc ion-dense spots with high zinc ion concentration, as discussed below. Nuclear expression of ZnT3 in primary and secondary oocytes was also observed, which is consistent with the results of a previous study [14, 16, 17]. Granulosa cells were less immunoreactive than those in a previous study [17], which may be due to antibodies.

In order to elucidate the function of ZnT3 in oocytes, we generated *ZnT3/Slc30a3* knockout (KO) mice. *ZnT3* KO mice have already been generated to elucidate zinc transport in the brain tissue [18]. However, the mouse strain generated in a previous study had a mixed background. To ensure genetic and phenotypic uniformity, we used genome-editing technology to generate the most widely used C57BL/6J mice. Exons 4 and 5 of the *ZnT3* gene were eliminated by a 638-bp deletion using the CRISPR/Cas9 system (Fig. 1B). The genetic deletion of *ZnT3* was confirmed by genome sequencing (Fig. 1B) and genotype analysis using genomic PCR, which showed bands of 259 and 435 bp for the KO and wild-type alleles, respectively (Fig. 1C). The homozygous deletion of the *ZnT3* gene did not result in embryonic lethality, which is in agreement with the results of a previous study [18].

Next, we examined whether ZnT3 protein expression was absent in *ZnT3* KO mice (Fig. 1D). ZnT3 is highly expressed in the synaptic vesicles of the brain [19, 20]. We confirmed the loss of ZnT3 protein expression in the brain and metaphase II (MII) oocytes of KO mice by western blot analysis and immunostaining (Fig. 1D and Supplementary

Received: April 26, 2024
Accepted: June 26, 2024
Advanced Epub: July 23, 2024

Correspondence: J Terakawa (e-mail: terakawa@azabu-u.ac.jp), J Ito (e-mail: itoj@azabu-u.ac.jp)

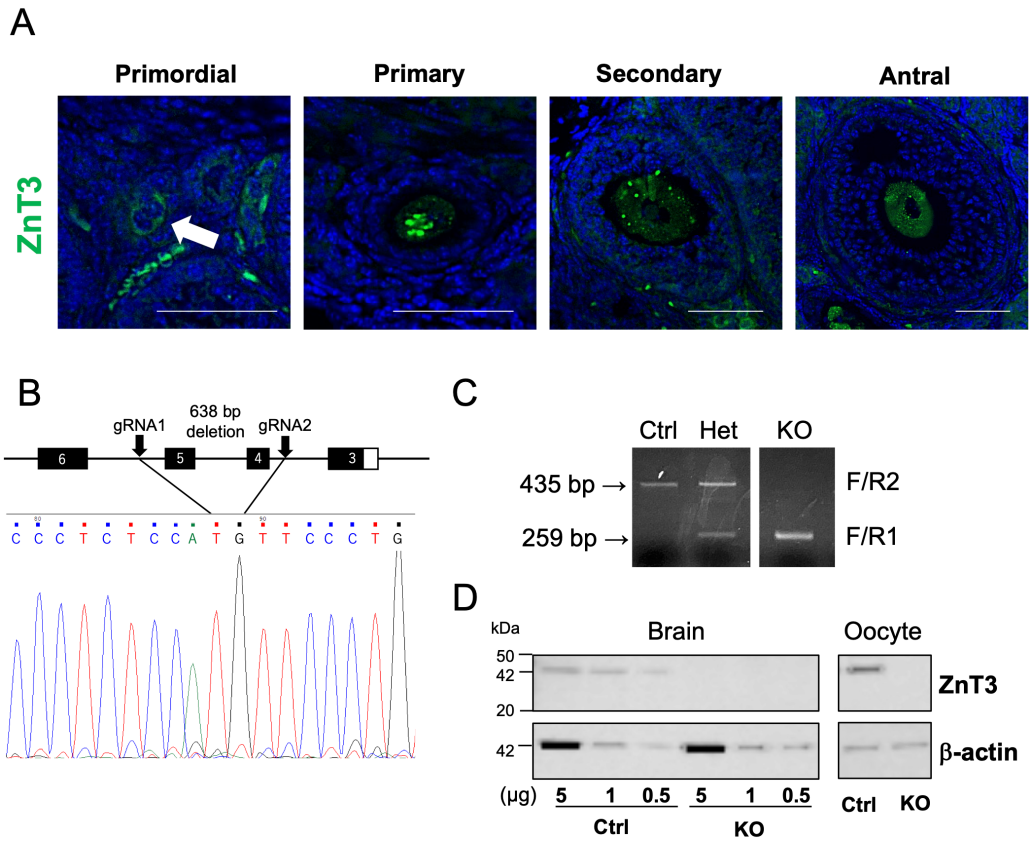


**Fig. 1.** Generation of *ZnT3* knockout mice. (A) The expression of ZNT3 in a mouse ovary. ZNT3 (green) is observed in oocyte cytoplasm but not in the plasma membrane surface. The blue shows nucleus. The arrow indicates a primordial follicular oocyte. The scale bars represent 50 μm. (B) Deletion mapping by Sanger sequencing analysis showed deletion of the 638-bp *ZnT3* gene including exon 4-5. (C) Genotyping of *ZnT3* alleles. Primers F and R1 amplified a 259-bp amplicon for the KO alleles, and primers F and R2 amplified a 435-bp amplicon for WT alleles. (D) Western blot analysis of the brain and oocytes from Ctrl and *ZnT3* KO mice. Concentrations of 0.5, 1, and 5 μg were applied to determine the amount of protein reacting with the anti-ZnT3 antibody in the brain. One hundred MII oocytes were used in order to detect oocyte expression. The expected molecular weight for ZNT3 is 42 kDa. Expression level of β-actin (42 kDa) served as a protein loading control. Molecular mass is indicated at the left.

Figs. 1 and 2).

To investigate the role of ZnT3 during fertilization, we measured the zinc ion levels in oocytes using FluoZin-3AM, fertilization, and blastocyst rates after *in vitro* fertilization. Mouse MII oocytes showed strong intensity of FluoZin-3AM, which may be due to the influx of zinc ions during oocyte maturation, as previously reported (Fig. 2A, Ctrl) [21, 22]; during the transition from MII to two-pronuclear (2PN) stage, the FluoZin-3AM signal was greatly reduced (Fig. 2A, Ctrl and KO), suggesting the occurrence of zinc sparks [23]. In contrast, *ZnT3* KO significantly reduced the intensity of FluoZin-3AM in MII oocytes and 2PN embryos compared to that in the controls (Fig. 2A). A previous study showed that the brains of *ZnT3* KO mice failed to accumulate zinc ions in synaptic vesicles, resulting in decreased zinc levels in the hippocampus and cortex [18]. Interestingly, the region of the high fluorescence intensity of FluoZin-3AM signals (zinc ion-dense spots) observed in the control oocytes was absent in the *ZnT3* KO (Fig. 2A, arrowheads). This suggests that this region may be a vesicle-like structure that accumulates zinc in the oocyte, including cortical granules, similar to synaptic vesicles. However, the details of this structure remain unclear because the localization of ZnT3 does not necessarily coincide with the region of high fluorescence intensity of the FluoZin-3AM signal. In CD-1 (ICR) oocytes, using the same zinc probe, dense regions of zinc ions were punctate and localized to the cortex; however, [14, 21] in C57BL/6J mouse oocytes, a larger dense region was characteristic of the localization of zinc accumulation (Supplementary Fig. 3). A more detailed analysis of the structures in this region will be required in the future. Since a reduction in the FluoZin-3AM signal from MII to 2PN was observed in *ZnT3* KO, zinc sparks were inferred to occur in the *ZnT3* KO, even though the total zinc level in the oocytes was lower than that in controls. Although cortical granules are thought to be the main source of zinc sparks [24], other mechanisms may exist that release zinc ions from the oocyte cytoplasm into the extracellular regions, in conjunction with our results.

After *in vitro* fertilization, the fertilization rate of oocytes from *ZnT3* KO females was 81.6%, which was similar to that of the Ctrl (73.2%; Fig. 2B, $P > 0.05$). Polyspermy was rarely observed in either groups (0.4% each). The subsequent blastocyst rates were also comparable between the *ZnT3* KO and Ctrl groups (75.0% and 76.1%, respectively). These results indicate that the reduced intercellular zinc ion levels induced by ZnT3 depletion in the oocytes did not affect sperm motility, fertilization, polyspermy prevention, or subsequent embryonic development. We tested the fertility of male and female *ZnT3* KO mice. The average litter size of the experimental groups was not significantly different: 7.6 pups (male Ctrl × female Ctrl), 5.6 pups (male Ctrl × female KO), 5.5 pups (male KO × female Ctrl), and 6.3 pups (male KO × female KO) ($P > 0.05$, Fig. 2C). These results indicate that the overall reproductive capacity was not

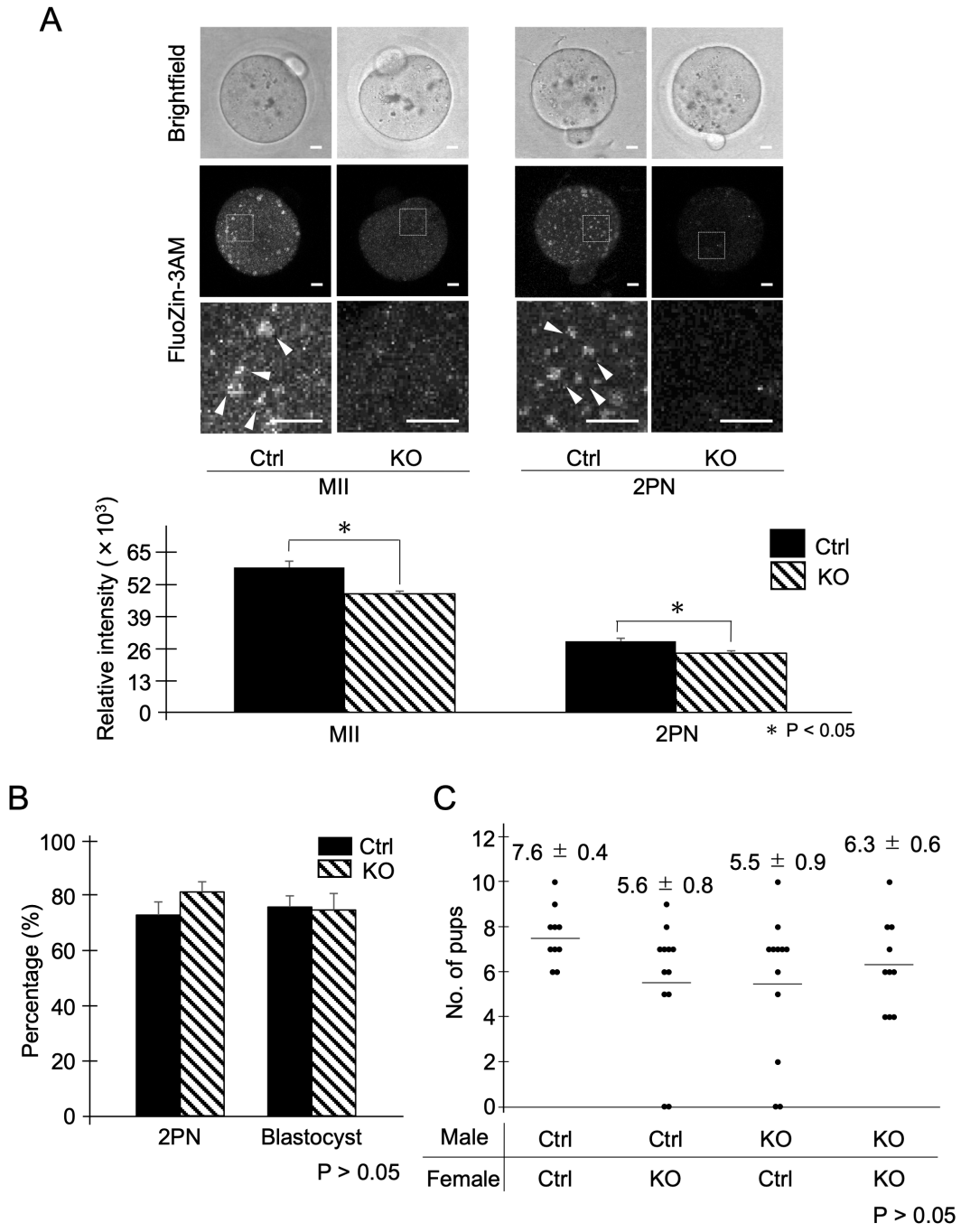


**Fig. 2.** The dynamics of zinc ions and the percentage of fertilization and embryonic development in *ZnT3* KO. (A) Comparison with the fluorescence intensity of FluoZin-3AM in MII oocytes and 2PN embryos. The upper panel shows a bright field. Representative fluorescence images are shown in the middle panel. The lower panel shows an enlarged white frame. White arrowheads point to clustering of FluoZin-3AM signals. The scale bars represent 10 µm. The lower graph shows the mean fluorescence intensity in oocytes or 2PN embryos. Data represent the averages ± SEMs of the experiments. For each experiment, 10–20 oocytes/embryos were stained and used for the measurement in each stage of the experiment, and these experiments were repeated three times. Statistical differences were calculated according to the Student's *t*-test. Different letters represent significant differences ($P < 0.05$). (B) The percentage of fertilized oocytes and developmental embryos. Data represent the averages ± SEMs of the experiments. These experiments were repeated at least three times. Statistical differences were calculated according to Student's *t*-test ($P > 0.05$; no significant difference). (C) Distribution of litter size with different combination of males and females. The average numbers of pups are represented by averages ± SEMs. The average numbers of pups were analyzed by one-way ANOVA ($P > 0.05$; no significant difference).

altered by ZnT3 deletion, which is consistent with the results of a previous study [18].

In summary, ZnT3 expressed in mouse oocytes plays an important role in the accumulation of zinc ions in oocytes. The total amount of zinc ions in the oocytes may not significantly affect fertilization and subsequent embryonic development. It has been reported that other zinc transporters such as ZnT1, ZnT4, and ZnT5 are expressed in mouse oocytes [14, 16]. However, the functions of other ZnTs in germ cells remain unclear, indicating the need for further investigation. The results of this study have demonstrated the variability of zinc

ions in oocytes and confirm the potential of *ZnT3* KO mice as a model for studying zinc ion dynamics not only in germ cells, as ZnT3 is known to play an important role in mouse brain function. Therefore, *ZnT3*-null mice (*Slc30a3*$^{em1Itj}$) established in this study are now available at RIKEN BRC (#RBRC12083) and will greatly contribute to the advancement of research on zinc-related cellular functions and diseases.

## Materials and Methods

All chemicals and reagents were purchased from Sigma-Aldrich (St. Louis, MO, USA) unless stated otherwise.

### *Animals*

The animals were housed in a barrier facility at the Azabu University. C57BL/6J female (4–8 weeks old) and male (8–12 weeks old) mice, and CD-1 (ICR) female mice (4–14 weeks old) were purchased from Charles River Laboratories Japan (Yokohama, Japan). The mice were housed under controlled lighting conditions (daily light period, 0600–1800 h). The study was approved by the Animal Experimentation Committee of Azabu University and was performed in accordance with the committee guidelines (200318-13 and 230309-1).

### *Immunofluorescent staining*

Immunofluorescence staining was performed as previously described with some modifications [25]. Ovaries were collected from sexually mature C57BL/6J female mice and fixed in 4% paraformaldehyde. Fixed ovaries were paraffin-embedded, and sections (6 µm) were deparaffinized, hydrated, and subjected to antigen retrieval by autoclaving in 10-mM sodium citrate buffer (pH 6.0) for 5 min. After blocking with Blocking One Histo (06349-64, Nacalai Tesque, Kyoto, Japan) for 1 h, the slides were incubated with primary antibody for rabbit anti-ZnT3 (1:100, 17363-1-AP, Proteintech, Rosemont, IL, USA) overnight at 4°C. The slides were incubated with Alexa Fluor 488 donkey anti-rabbit IgG (H+L)-conjugated secondary antibodies (1:500, Jackson ImmunoResearch Laboratories, West Grove, PA, USA) for 1 h and mounted with ProLong Glass Antifade Mountant with NucBlue Stain (P36981, Thermo Fisher Scientific, Waltham, MA, USA). Micrographs were obtained using a BZ-X700 microscope (Keyence, Tokyo, Japan).

### *Oocyte preparation*

In order to obtain MII oocytes, C57BL/6J female mice were intraperitoneally injected with 5 IU equine chorionic gonadotropin (eCG; Serotropin; ASKA Animal Health, Tokyo, Japan), followed by an injection with 5 IU human chorionic gonadotropin (hCG; Gonatropin; ASKA Pharmaceutical, Tokyo, Japan) 48 h later. Cumulus-oocyte complexes (COCs) were collected from the oviductal ampulla 14–16 h after the hCG injection.

### *In vitro fertilization (IVF)*

IVF and sperm collection was performed using a modified version of the method described in our previous study [26]. In brief, ovulated COCs-MII were preincubated for 1 h in 80 µl human tubal fluid (HTF) droplets supplemented with 1.25-mM reduced glutathione. Frozen-thawed sperm suspensions were suspended in 200 µl preincubation medium (HTF containing 0.4-mM methyl-β-cyclodextrin) and 0.1-mg/ml polyvinyl alcohol (PVA), but without bovine serum albumin, and were incubated at 37°C under 5% $CO_2$ in humidified air for 1 h. The preincubated spermatozoa were added to HTF medium droplets containing oocytes (final concentrations of 2.0 ×$10^6$ sperm/ml) and then co-cultured for 6 h. After the culture, cumulus cells of oocytes were removed using a fine glass pipette and transferred into 50 µl KSOMaa medium. They were cultured at 37°C under 5% $CO_2$ in humidified air for approximately 24–96 h.

### *Generation of ZnT3 knockout mice*

CRISPR-mediated removal of exons 4 and 5 of the *ZnT3* gene from the genomic DNA was performed using fertilized eggs. The target sequences of the guide RNA (gRNA#1, ATCTGCTGTAGGTCCGAGTG and gRNA#2, GAACATCTAGAAGGTCGGAC) were designed using CRISPOR (http://crispor.tefor.net) [27] and purchased as an crRNA product from Integrated DNA Technologies (IDT, Coralville, IA, USA). Fertilized pronuclear-stage embryos were prepared using IVF. The complexes of crRNAs (2 µM each), tracrRNA (4 µM) and Cas9 protein (100 ng/µl) (IDT) in Opti-MEM™ I Reduced Serum Medium (31985062, Thermo Fisher Scientific) were then introduced into pronuclear-stage embryos by electroporation as previously described [28]. Electroporated embryos were washed and cultured overnight in the KSOMaa medium. The 2-cell embryos were transplanted into pseudo-pregnant recipient CD-1 (ICR) mice. Pups from transplanted embryos were considered the F0 generation. The tail tips of 2-week-old F0 mice were excised and lysed using DirectPCR Lysis Reagent (102-T, Viagen Biotech, LA, USA) with proteinase K (161-28701, FujiFilm Wako Pure Chemicals, Osaka, JAPAN). Genotypes were confirmed by polymerase chain reaction (PCR) using the following primers: GCACATCCAATGACGACAAC (F1), GGGGAGGTGGTTGGTAAGTT (R1), and CCTCTTTTCCCTCTGGCTTT (R2). The PCR cycle consisted of an initial denaturation at 98°C for 5 min, followed by 30 cycles of 98°C (10 sec), 58°C (30 sec), and 72°C (40 sec) with a final extension at 72°C (5 min). A combination of F1 and R1 detected mutant alleles (approximately 259 bp), whereas F1 and R2 detected wild-type alleles (435 bp). F0 mice were backcrossed with wild-type C57BL/6J mice to obtain the F1 generation and confirm germline transmission. An F1 line carrying a 638-bp deletion, removing the region flanked by gRNA#1 and gRNA#2, was intercrossed to obtain homozygous *ZnT3*-null mice. *ZnT3*-null mice (*Slc30a3*$^{em1Itj}$) are now available at RIKEN BRC (#RBRC12083).

### *Western blotting*

Western blotting was performed as previously described [29] with some modifications. Whole brains and a hundred MII oocytes were lysed in the Laemmli sample buffer (Bio-Rad Laboratories, Hercules, CA, USA) containing 5% 2-mercaptoethanol. Samples were separated on 8% Bis-Tris gels using sodium dodecyl sulfate-polyacrylamide gel electrophoresis and transferred to PVDF membranes (Bio-Rad Laboratories). The PVDF membranes were blocked in 10% skim milk (FujiFilm Wako Pure Chemicals) in Tris-buffered saline with 0.1% Tween-20 (Yoneyama Yakuhin Kogyo, Osaka, Japan) and probed overnight with primary antibody to rabbit anti-ZnT3 (1:1,000; 17363-1-AP, Proteintech) or to monoclonal mouse anti-β-actin (1:5,000; A5316, Sigma-Aldrich) at 4°C. The membranes were incubated with the secondary antibody, horseradish peroxidase-conjugated anti-rabbit IgG (1:5,000; Cell Signaling Technology, Danvers, MA, USA), or horseradish peroxidase-conjugated anti-mouse IgG (1:5,000; Cell Signaling Technology) for 1 h at room temperature. After the membranes were washed, the immunoreactive proteins were visualized using the ECL™ Western Blotting Analysis System (Cytiva, Tokyo, Japan) according to the manufacturer's recommendations. Signals were captured using an ImageQuant LAS 4000 (Cytiva).

*Intracellular zinc ion detection*

FluoZin3-AM staining was performed as described previously [23]. The collected MII and 2PN were loaded in 50 µl of medium that was suitable for each stage containing FluoZin3-AM (2 µM; F24195, Thermo Fisher Scientific) at 37°C under 5% $CO_2$ in humidified air for 1 h, and then observed with a TCS SP5 II confocal microscope (Leica Microsystems, Wetzlar, Germany). The pixel intensity per unit area after background subtraction was determined in MII and 2PN using the ImageJ image-processing software.

*Fertility test*

Sexually mature male Ctrl or *ZnT3* KO mice were caged with sexually mature Ctrl or *ZnT3* KO female mice. Copulation was confirmed by checking for vaginal plugs every morning (0900–1100 h). Plugged females were separated and monitored during pregnancy. The number of pups was counted after parturition (20–21 days after plug confirmation).

*Statistical analysis*

Values from three or more trials were used to evaluate statistical significance. Statistical analyses were performed using Statcel 3 software (OMS Ltd., Saitama, Japan). For the fluorescence intensity of FluoZin-3 AM, the rates of fertilization and embryo development were evaluated statistically using the Student's *t*-test. Fertilization and embryo development parameters, calculated as percentages, were subjected to arcsine transformation before Student's *t*-tests were performed. The average number of pups was analyzed using one-way ANOVA. Values are shown as means ± standard errors of the mean (SEMs), and differences were considered significant at P values < 0.05.

**Conflict of interests:** The authors have no potential conflicts of interest to declare.

## Acknowledgments

This research was supported by Grants-in-Aid for Scientific Research from the Japan Society for the Promotion of Science (JSPS) (KAKENHI, 21H02384 and 20H05373 to J.I., 21K09512 to J.T., 22H04268 and 24H02601 to A.K.) and the Sasakawa Scientific Research Grant from the Japan Science Society (2019-4044) to A.K., (2024-4093) to H.S. This study was also funded by the Center for Diversity, Equity, and Inclusion at Azabu University (H.S.). This research was partially supported by the Center for Human and Animal Symbiosis Science, Azabu University and a research project grant awarded by the Azabu University Research Services Division.

## References

1. **Suzuki M, Suzuki T, Watanabe M, Hatakeyama S, Kimura S, Nakazono A, Honma A, Nakamaru Y, Vreugde S, Homma A.** Role of intracellular zinc in molecular and cellular function in allergic inflammatory diseases. *Allergol Int* 2021; **70**: 190–200. [Medline] [CrossRef]
2. **MacDonald RS.** The role of zinc in growth and cell proliferation. *J Nutr* 2000; **130**(Suppl): 1500S–1508S. [Medline] [CrossRef]
3. **Jackson KA, Valentine RA, Coneyworth LJ, Mathers JC, Ford D.** Mechanisms of mammalian zinc-regulated gene expression. *Biochem Soc Trans* 2008; **36**: 1262–1266. [Medline] [CrossRef]
4. **Bernhardt ML, Kong BY, Kim AM, O'Halloran TV, Woodruff TK.** A zinc-dependent mechanism regulates meiotic progression in mammalian oocytes. *Biol Reprod* 2012; **86**: 114. [Medline] [CrossRef]
5. **Suzuki T, Yoshida N, Suzuki E, Okuda E, Perry ACF.** Full-term mouse development by abolishing Zn2+-dependent metaphase II arrest without Ca2+ release. *Development* 2010; **137**: 2659–2669. [Medline] [CrossRef]
6. **Ohe M, Kawamura Y, Ueno H, Inoue D, Kanemori Y, Senoo C, Isoda M, Nakajo N, Sagata N.** Emi2 inhibition of the anaphase-promoting complex/cyclosome absolutely requires Emi2 binding via the C-terminal RL tail. *Mol Biol Cell* 2010; **21**: 905–913. [Medline] [CrossRef]
7. **Kim AM, Bernhardt ML, Kong BY, Ahn RW, Vogt S, Woodruff TK, O'Halloran TV.** Zinc sparks are triggered by fertilization and facilitate cell cycle resumption in mammalian eggs. *ACS Chem Biol* 2011; **6**: 716–723. [Medline] [CrossRef]
8. **Que EL, Duncan FE, Lee HC, Hornick JE, Vogt S, Fissore RA, O'Halloran TV, Woodruff TK.** Bovine eggs release zinc in response to parthenogenetic and sperm-induced egg activation. *Theriogenology* 2019; **127**: 41–48. [Medline] [CrossRef]
9. **Duncan FE, Que EL, Zhang N, Feinberg EC, O'Halloran TV, Woodruff TK.** The zinc spark is an inorganic signature of human egg activation. *Sci Rep* 2016; **6**: 24737. [Medline] [CrossRef]
10. **Seeler JF, Sharma A, Zaluzec NJ, Bleher R, Lai B, Schultz EG, Hoffman BM, LaBonne C, Woodruff TK, O'Halloran TV.** Metal ion fluxes controlling amphibian fertilization. *Nat Chem* 2021; **13**: 683–691. [Medline] [CrossRef]
11. **Que EL, Duncan FE, Bayer AR, Philips SJ, Roth EW, Bleher R, Gleber SC, Vogt S, Woodruff TK, O'Halloran TV.** Zinc sparks induce physiochemical changes in the egg zona pellucida that prevent polyspermy. *Integr Biol (Camb)* 2017; **9**: 135–144. [Medline] [CrossRef]
12. **Hara T, Yoshigai E, Ohashi T, Fukada T.** Zinc transporters as potential therapeutic targets: An updated review. *J Pharmacol Sci* 2022; **148**: 221–228. [Medline] [CrossRef]
13. **Lichten LA, Cousins RJ.** Mammalian zinc transporters: nutritional and physiologic regulation. *Annu Rev Nutr* 2009; **29**: 153–176. [Medline] [CrossRef]
14. **Kong BY, Duncan FE, Que EL, Kim AM, O'Halloran TV, Woodruff TK.** Maternally-derived zinc transporters ZIP6 and ZIP10 drive the mammalian oocyte-to-egg transition. *Mol Hum Reprod* 2014; **20**: 1077–1089. [Medline] [CrossRef]
15. **Chen YH, Kim JH, Stallcup MR.** GAC63, a GRIP1-dependent nuclear receptor coactivator. *Mol Cell Biol* 2005; **25**: 5965–5972. [Medline] [CrossRef]
16. **Chen YY, Chen S, Ok K, Duncan FE, O'Halloran TV, Woodruff TK.** Zinc dynamics regulate early ovarian follicle development. *J Biol Chem* 2023; **299**: 102731. [Medline] [CrossRef]
17. **Zhong ML, Guo C, Chi ZH, Shan ZY, Teng WP, Wang ZY.** Distribution of zinc and zinc transporters in the mouse ovarian follicles and corpus luteum. *Histol Histopathol* 2013; **28**: 1517–1527. [Medline]
18. **Cole TB, Wenzel HJ, Kafer KE, Schwartzkroin PA, Palmiter RD.** Elimination of zinc from synaptic vesicles in the intact mouse brain by disruption of the ZnT3 gene. *Proc Natl Acad Sci USA* 1999; **96**: 1716–1721. [Medline] [CrossRef]
19. **Chacon J, Rosas L, Cuajungco MP.** ZnT3 expression levels are down-regulated in the brain of Mcoln1 knockout mice. *Mol Brain* 2019; **12**: 24–3. [Medline] [CrossRef]
20. **Shen H, Zhang Y, Xu J, Long J, Qin H, Liu F, Guo J.** Zinc distribution and expression pattern of ZnT3 in mouse brain. *Biol Trace Elem Res* 2007; **119**: 166–174. [Medline] [CrossRef]
21. **Kim AM, Vogt S, O'Halloran TV, Woodruff TK.** Zinc availability regulates exit from meiosis in maturing mammalian oocytes. *Nat Chem Biol* 2010; **6**: 674–681. [Medline] [CrossRef]
22. **Kong BY, Duncan FE, Que EL, Xu Y, Vogt S, O'Halloran TV, Woodruff TK.** The inorganic anatomy of the mammalian preimplantation embryo and the requirement of zinc during the first mitotic divisions. *Dev Dyn* 2015; **244**: 935–947. [Medline] [CrossRef]
23. **Kageyama A, Suyama A, Kinoshita R, Ito J, Kashiwazaki N.** Dynamic changes of intracellular zinc ion level during maturation, fertilization, activation, and development in mouse oocytes. *Anim Sci J* 2022; **93**: e13759. [Medline] [CrossRef]
24. **Que EL, Bleher R, Duncan FE, Kong BY, Gleber SC, Vogt S, Chen S, Garwin SA, Bayer AR, Dravid VP, Woodruff TK, O'Halloran TV.** Quantitative mapping of zinc fluxes in the mammalian egg reveals the origin of fertilization-induced zinc sparks. *Nat Chem* 2015; **7**: 130–139. [Medline] [CrossRef]
25. **Namiki T, Terakawa J, Karakama H, Noguchi M, Murakami H, Hasegawa Y, Ohara O, Daikoku T, Ito J, Kashiwazaki N.** Uterine epithelial Gp130 orchestrates hormone response and epithelial remodeling for successful embryo attachment in mice. *Sci Rep* 2023; **13**: 854. [Medline] [CrossRef]
26. **Kageyama A, Tsuchiya M, Terakawa J, Ito J, Kashiwazaki N.** A combined treatment with progesterone, anti-inhibin serum, and equine chorionic gonadotropin improves number of ovulated oocytes in young C57BL/6J mice. *J Reprod Dev* 2023; **69**: 223–226. [Medline] [CrossRef]
27. **Concordet JP, Haeussler M.** CRISPOR: intuitive guide selection for CRISPR/Cas9 genome editing experiments and screens. *Nucleic Acids Res* 2018; **46**(W1): W242–W245. [Medline] [CrossRef]
28. **Kaneko T.** Genome editing in mouse and rat by electroporation. *Methods Mol Biol* 2017; **1630**: 81–89. [Medline] [CrossRef]
29. **Ito J, Yoshida T, Kasai Y, Wakai T, Parys JB, Fissore RA, Kashiwazaki N.** Phosphorylation of inositol 1,4,5-triphosphate receptor 1 during in vitro maturation of porcine oocytes. *Anim Sci J* 2010; **81**: 34–41. [Medline] [CrossRef]